Preparation of high-surface-area activated carbon from *Zizania latifolia* leaves by one-step activation with K_2CO_3/rarefied air

D. C. Huang · Q. L. Liu · W. Zhang · J. Ding · J. J. Gu · S. M. Zhu · Q. X. Guo · D. Zhang

Abstract An activated carbon (AC) with high-porosity was prepared from *Zizania latifolia* leaves by a one-step method combining chemical and physical activation. K_2CO_3 was employed as a chemical reagent, and air as a physical agent. During the activation, several key parameters were discussed, including the effects of activation temperature, K_2CO_3 impregnation ratio, amount of introduced air on the surface area and pore volumes evolution of the ACs derived from the *Zizania latifolia* leaves. The synergistic effect between the chemical agent and the physical agent was also investigated. Under optimal activation conditions, the as-synthesized AC attained a maximum surface area up to 2481 m^2/g, with 1.21 cm^3/g pore volume, and it had a micro/meso porosity developed by the combining activation. The crystal sizes of the as-synthesized AC along the *a*- and *c*-axes were about 5 nm and 1–2 nm, respectively. The average thickness of the crystallites is 3–4 layers with about 0.37 nm interlayer spacing.

Introduction

Activated carbon (AC), because of its large internal surface area and high degree of porosity [1], is widely used in separation, purification, and catalyst supporting [2–8] for the porous structure. Abundant availability and low cost of agricultural by-products, such as rice hull, nutshells, and fruit stones, make them good candidates and sources of raw materials for ACs [9–11].

For the preparation of AC, activation conditions and activation methods are mostly investigated since they are principal factors to determine the pore size distribution, pore shape, and surface chemistry [5, 12–14]. Basically, AC can be produced by two methods: physical activation and chemical activation [15, 16].

Physical activation normally involves pyrolysis and activation. During pyrolysis, the starting materials are made into chars with rudimentary pore structures in an inert atmosphere. These chars are then activated in oxidation gases (e.g. steam and carbon dioxide) at 800–1000 °C to produce the final AC [17–19]. Chemical activation is known as a single step method to prepare AC using chemical agents such as alkali and alkaline earth metal containing substances and some acids such as KOH, K_2CO_3, NaOH, Na_2CO_3, $ZnCl_2$, $MgCl_2$, H_3PO_4, and H_2SO_4 [20–24]. The temperature is lower with less time compared with physical activation. Moreover, AC porous structure is better developed with chemical activation [19, 25, 26].

Much work has been done to develop a new activation method [27, 28] including two steps: (1) the chemical activation of the starting materials with KOH, K_2CO_3; (2) the physical activation of the chemically activated AC by using carbon dioxide or steam. However, very few literatures mentioned about one-step physical/chemical activation that combined these two activations simultaneously.

In this work, one-step K_2CO_3/air activation was employed to produce ACs with high specific surface area, and the agricultural residues, *Zizania latifolia* leaves, were chosen as the raw material which has different chemical composition from the usual sources, such as coconut shell, rice husk soybean shells, and etc. The optimal activation conditions and the

D. C. Huang · Q. L. Liu · W. Zhang · J. Ding ·
J. J. Gu · S. M. Zhu · D. Zhang (✉)
State Key Lab of Metal Matrix Composites, Shanghai Jiao Tong
University, Shanghai 200030, People's Republic of China
e-mail: zhangdi@sjtu.edu.cn

Q. X. Guo
Department of Electrical and Electronic Engineering,
Saga University, Honjo-1, Saga 840-8502, Japan

synergistic effect between K_2CO_3 and diluted air would be investigated. Moreover, the pore structure (specific surface area and pore volume), morphologies, and nanotexture of the as-synthesized AC would also be characterized.

Experiments

Materials

The *Zizania latifolia* leaves used in this study as a raw material were collected from Qingpu District in Shanghai, China, and the chemical composition of *Zizania latifolia* leaves was given in Table 1. The *Zizania latifolia* leaves were dried in air, grounded in a high-speed rotary cutting mill, and then particles with 0.6–1.8 mm diameter were selected for the activation.

Preparation of ACs

The physical/chemical activation was carried out in following steps:

(i) *Zizania latifolia* leaves and chemical activation reagent (K_2CO_3) were mixed for 6 h under continuous agitation.
(ii) This mixture was dried at 110 °C for 12 h to prepare the impregnated sample.
(iii) The impregnated sample was set in a stainless steel reactor, heated to the activation temperatures with 10 °C/min heating rate, and then the system was held for 2 h with airflow before cooling down in vacuum. The airflow rate ranged from 0 to 120 mL/min, and the corresponding partial pressure of air was 0–15 Pa.
(iv) The carbonized samples were washed several times with HCl solution, and then distilled water to remove impurities and reduce the amount of ash content of the ACs.

Physical activation and chemical activation were also employed for comparison. The processes of physical activation and chemical activation were similar to that of physical/chemical activation, except that the impregnation of K_2CO_3 was skipped in the physical activation, and that no air was introduced in the chemical activation.

The ACs prepared by physical activation, chemical activation, and physic/chemical activation were, respectively, denoted as P-AC-*xxx*, C-AC-*xxx*, and PC-AC-*xxx*, in which the "*xxx*" represented the heat treatment temperature (HTT) of the referred AC.

Characterization of the prepared AC

The characteristic of the pore structure of the resulting ACs was determined by nitrogen adsorption at 77 K, using an automatic adsorption instrument. Prior to gas adsorption measurements, the samples were degassed at 250 °C under vacuum for 6 h. The surface area, pore volume, and pore size distribution of the ACs were determined by the application of the Brunauer–Emmett–Teller (BET) and *t*-plot analysis software. The BET surface area (S_{BET}) was assessed by applying relative pressure ranging from 0.01 to 0.15. The total pore volumes (V_{tot}, cm^3/g) were estimated to be the liquid volumes of N_2 at a high relative pressure. The *t*-plot method was applied to the micropore volume (V_{mi}), and the mesopore volume (V_{me}) was obtained by subtracting the micropore volume from the total pore volume. The morphologies of the ACs produced from *Zizania latifolia* leaves were observed at the voltage of 20 kV by field emission scanning electron microscope (FE-SEM). Nanotexture of the ACs was investigated by a high-resolution transmission electron microscopy (HRTEM) operating at 200 kV. The crystallite and sizes were identified ($CuK_\alpha = 1.542$ Å) by X-ray diffraction (XRD). The scan speed was 1°/min. Estimation of mean crystallite sizes along the *a*-axis (L_a) and *c*-axis (L_c) could be generally obtained from powder XRD data by the following equations [29]:

$$L_c = 0.90\lambda/\beta \cos \theta_{002} \qquad (1)$$

$$L_a = 1.94\lambda/\beta \cos \theta_{10} \qquad (2)$$

where λ is 0.1542 nm and β is the peak width at half height.

Table 1 Chemical composition of *Zizania latifolia* leaves

Ingredient	Content (wt%)
Cellulose	20.6
Hemicellulose	26.1
Lignin	17.5
Ash	1.9
Protein	1.5
Starch	7.1
Moisture	11.4
Others	13.9

Results and discussions

The optimum conditions for preparing AC

The influence of carbonization temperature on the surface area and pore volume

Heat treatment temperature (HTT) plays an important role in the pyrolysis of the precursors so it is a key parameter for the surface area and the pore volume of the AC. The

Table 2 Surface areas, pore volumes, and yield of P-AC, C-ACs, and PC-ACs at different final carbonization temperatures

Temperature (°C)	Activation	S_{BET} (m²/g)	V_{tot} (m³/g)	V_{me} (m³/g)	V_{mi} (m³/g)	S_{me} (m²/g)	S_{mi} (m²/g)	Yield (%)
700	Physical	247	–	–	–	–	–	25.3
800		637	0.44	0.13	0.31	43	594	23.9
900		756	0.5	0.15	0.36	63	693	19.8
1100		233	–	–	–	–	–	15.7
800	Chemical	1390	0.69	0.22	0.47	361	1029	27.7
850		1626	1.16	0.46	0.7	456	1170	23.4
900		1484	0.75	0.26	0.49	417	1067	21.3
700	Physical/Chemical	603	0.21	0.05	0.16	73	530	21.9
800		1761	1.19	0.36	0.83	214	1547	16.9
850		2481	1.21	0.32	0.89	651	1831	13.3
900		2090	0.97	0.31	0.66	475	1615	10.8

effects of HTT on the BET surface area (S_{BET}) and pore volumes of the ACs are shown in Table 2.

Heat treatment temperature (HTT) had a similar influence on both physical and chemical activation. At lower activation temperature, the growth of HTT helped improving the development of porous structure of AC, while at higher activation temperature, the S_{BET} of the AC decreased while HTT increased. For the C-AC, the maximum S_{BET} of 1626 m²/g was obtained at HTT of 850 °C. Surface areas of micropores (S_{mi}) and mesopores (S_{me}) of C-AC-850 were 1170 m²/g and 456 m²/g, while the V_{tot}, V_{mi}, and V_{me} of the C-AC-850 were 1.16, 0.46, and 0.70 cm³/g, respectively. For P-AC, the maximum S_{BET} of was obtained at HTT of 900 °C. Other researchers who used H_2O, CO_2 as activation reagents [30, 31] obtained similar conclusions.

For PA-ACs, their surface areas and pore volumes also gradually increased at first and then decreased with the increscence of HTT. The S_{BET} of the PC-AC-850 showed the maximum value of 2481 m²/g due to the activation of K_2CO_3 and O_2 in the introduced air. If the HTT was more than 850 °C, the value of S_{BET} of the PC-AC would decrease from the maximum value. When HTT was 900 °C, the S_{BET} of the PC-AC was 2090 m²/g.

The porous structure of the PC-AC was developed by chemical activation, physical activation, and the possible synergistic effect between chemical activation agent and physical activation agent. During the carbonization, a dehydration of the raw material happened below 550 °C, resulting in charring and aromatization of the carbon skeleton [32, 33]. When the HTT ranged from 550 to 850 °C, the S_{BET} of the PC-ACs increased significantly with the activation temperature rising, since high temperature would improve the activity of O_2 and K_2CO_3 in the C–O_2 reaction and C–K_2CO_3 reaction. The physical and chemical activation created large numbers of new pores in the samples by

continuous devolatilization of the chars and carbon burnoff, and enhanced the existing pores, meanwhile the yield decreased from 21.9 to 13.3 wt%. At 850 °C, the S_{BET} of the PC-AC reached the maximum of 2481 m²/g, much higher than that of C-AC-850. The introduced air could improve the porous structure of the PC-AC during the chemical activation. It should be noted that the introduced air causes much burnoff, and that the yield of the PC-AC-850 (13.3 wt%) was much lower than that of C-AC-850 (23.4 wt%). Beyond 850 °C, the activity of the O_2, K_2CO_3, and the carbon skeleton increased. The C–O_2 reaction and C–K_2CO_3 reaction created new micropores but the reactions rapidly gave rise to the collapse of the wall of the micropore and the combination of the micropores, which would decrease the S_{BET} and yield of the PC-AC. Moreover, heat shrinkage at higher temperature [9] would also lead to a decrease in surface area and micropore volume.

The influence of impregnation ratio on the surface area and pore volume

The effects of impregnation ratio on S_{BET}, and micropore volume of ACs were given in Fig. 1. Figure 2 showed the nitrogen adsorption–desorption isotherm for ACs prepared by applying various impregnation ratios. The experimental impregnation ratio was estimated from the following equation:

$$R_i = \frac{W_i - W_z}{W_z} \qquad (3)$$

where R_i is the impregnation ratio, W_z is the weight of the *Zizania latifolia* leaves, and W_i is the weight of the *Zizania latifolia* leaves after impregnation.

The activation of K_2CO_3 was carried out by the reaction between K_2CO_3 and the char. Above 700 °C, K_2CO_3 would react with the char, as expressed in Eq. 4

Fig. 1 Surface areas and pore volumes of PC-ACs at different impregnation ratios (airflow rate = 100 mL/min)
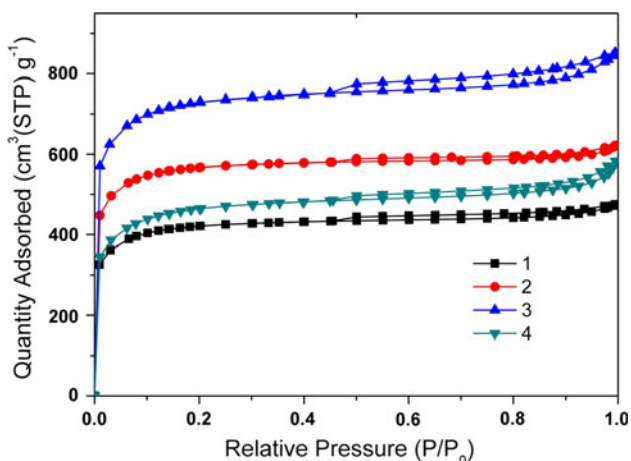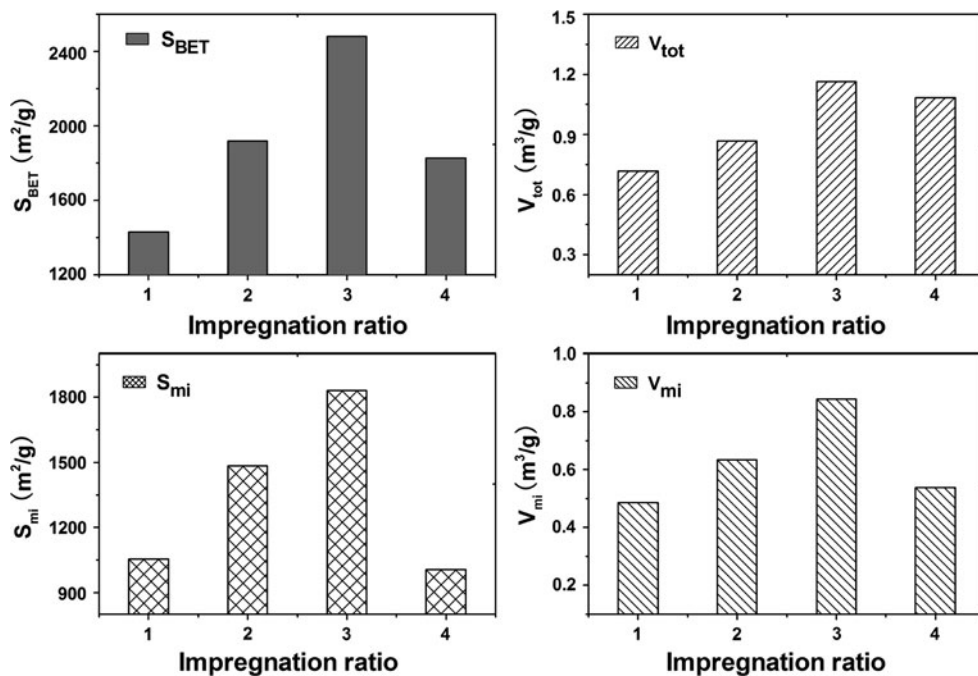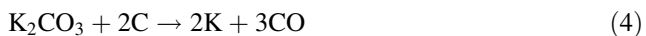

Fig. 2 Nitrogen adsorption–desorption isotherms for prepared PC-ACs with variable impregnation ratio (rate flow rate = 100 mL/min)

$$K_2CO_3 + 2C \rightarrow 2K + 3CO \qquad (4)$$

At higher temperature, the K_2CO_3 was reduced to metallic potassium, and then the metallic potassium penetrated to the carbon skeleton. The alkaline metal carbonate would be decomposed at the temperature below the melting point, increasing the pore volume.

The BET surface area of the ACs increased while adjusting the impregnation ratio from 1.0 to 3.0, which means that, for an impregnation ratio of 1.0, the carbon loss due to the C–K_2CO_3 reaction was not high enough to maximize the S_{BET}. With an impregnation ratio of 3.0, the S_{BET} of the as-synthesized AC reached the maximum value. For the impregnation ratio above 3.0, excessive

attack of the chemicals to the carbon skeleton led to additional gasification of carbon, widening some of the pores or even collapsing the walls of carbon, so that the S_{BET} and the V_{mi} decreased from 2481 to 1827 m^2/g and 0.89 to 0.54 m^3/g, respectively

The influence of the air amount on the surface area and pore volume

The effect of air on activation was also investigated by the experiments with different airflow rates, and the experiments were carried out with uniform impregnation ratio of 3.0 and the HTT of 850 °C. The results of surface areas and pore volumes of the PC-ACs are shown in Fig. 3. The nitrogen adsorption–desorption isotherms for ACs prepared by applying various air amounts are given in Fig. 4.

The surface areas and pore volumes of the AC increased rapidly when the air flow rate increased from 0 to 100 mL/min, and the PC-AC prepared at the flow rate of 100 mL/min had the highest S_{BET} of 2481 m^2/g. During the activation of PC-AC, except for direct physical activation, the involved O_2 also developed the porous structure of the PC-AC by a synergistic effect of K_2CO_3/O_2 activation. As discussed before, K_2CO_3 reacted with carbon skeleton and formed alkaline metal carbonate, and then, the decomposition of the alkaline metal carbonate increased the pore volume of the AC. During the physical/chemical activation, the introduced air would favor the formation of potassium oxide, so the air enhanced the chemical activation of K_2CO_3, and further improved the surface area and porous structure of the PC-AC.
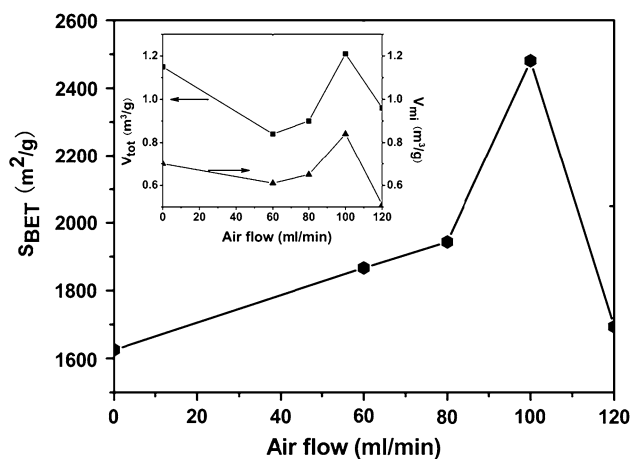
Fig. 3 Surface areas and pore volumes of PC-ACs at different airflow rates (impregnation ratio = 3.0)
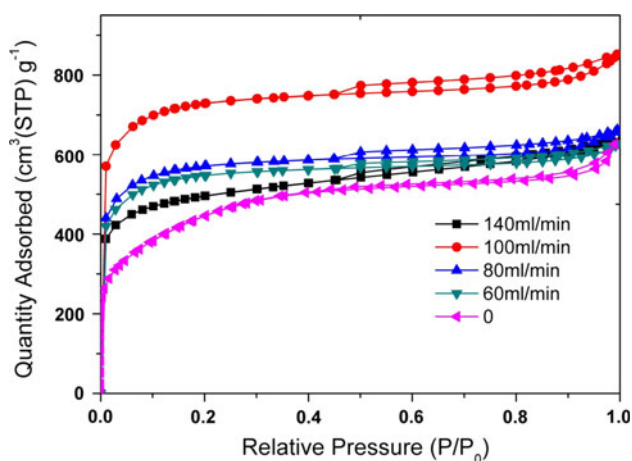

Fig. 4 Nitrogen adsorption–desorption isotherms for prepared ACs with variable airflow (impregnation ratio = 3.0)

When the air flow was higher than 100 mL/min, the S_{BET} and microporous volume decreased due to the excessive reaction between O_2 and porous carbon skeleton. When the introduced air increased from 100 to 120 mL/min, the S_{BET} decreased from 2482 to 1694 m^2/g, and the total pore volume and microporous volume decreased from 1.21 to 0.90 m^3/g to 0.89 to 0.51 m^3/g, respectively.

The appropriate amount of air could enhance the chemical activation of K_2CO_3 and improve the porous structure of AC. The AC made by physic/chemical activation with different amount of air flow rate had BET surface areas from around 1700 m^2/g to more than 2400 m^2/g. Such high-surface areas are competitive comparable to commercially produced ACs which typically ranges from 500 to 2000 m^2/g [34].

In Fig. 7, a rapid increase in the adsorption–desorption isotherms is observed at low relative pressure, which is followed by a nearly horizontal plateau at higher relative

pressures. Those isotherms are S-type curves, fitting the type II isotherm based on the classification of the Brunauer, Deming, Deming and Teller (BDDT). The type II isotherms indicate that besides micropores, the perpared ACs included some macropores.

The morphology of the as-synthesized AC

The SEM images of P-AC and PC-AC were given in Fig. 5. As shown in Fig. 5a, the P-AC had a porous structure with the pore diameters ranging in 2–5 μm, which were mainly replicated from the natural structure of the *Zizania latifolia* leaves. In the physical/chemical activation (in Fig. 5b), heat shrinkage and the reactions between agents and carbon led to the collapse of the carbon walls, and destroyed the micrometer-sized porous structure which could be seen in the P-AC structures. However, the physical/chemical activation successfully developed the porous structure of the PC-AC which was activated under the optimal activation conditions (carbonization temperature of 850 °C, impregnation ratio of 3.0, and the air pressure of 55 Pa), shown in the magnified figure of the PC-AC (in Fig. 5c).

The nanotexture of the as-synthesized AC

X-ray diffraction (XRD) pattern of the PC-AC-850 is given in Fig. 6. The two peaks are formed due to the diffraction from (002) and (10) planes. Based on Bragg's Law, $d_{(002)}$, the interlayer spacing of the plane (002), was 0.37 nm, among the average range between 0.35 and 0.37 for ACs [35–38]. L_a was 5.4 nm, and L_c was 1.1 nm. Therefore, in the as-synthesized PC-AC, the thickness of the crystallites is mostly about 3–4 layers. In the small crystallite, the interaction of carbon atoms in adjacent layers would lead to lattice strain which expanded the interlayer spacing, so the value of $d_{(002)}$ of the PC–AC was larger than that of graphite (0.335 nm).

Figure 7 shows the interior structure of the PC-AC. The structure was disordered and isotropic, consisting of small, curled, and tightly packed carbon layers. The carbon layers were typically 1–2 nm thick and 5 nm in length, enclosing randomly shaped pores with diameter less than 1 nm. The sizes of the carbon layers are approximately consistent with results obtained by XRD. The inset image in Fig. 7 is the electron-diffraction pattern of the PC-AC. There were no obvious diffraction rings, confirming that the nanotexture of the PC-AC was not well crystallized.

Conclusions

The one-step physical/chemical activation is an effective method for producing highly porous AC. The AC produced

Fig. 5 Morplogies of **a** P-AC (HTT = 900 °C. airflow rate = 100 mL/min), **b** and **c** PC-AC (HTT = 850 °C. Impregnation ratio = 3. Airflow rate = 100 mL/min)
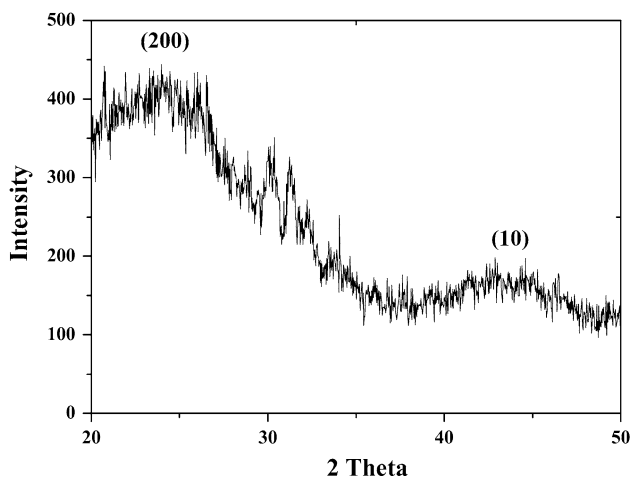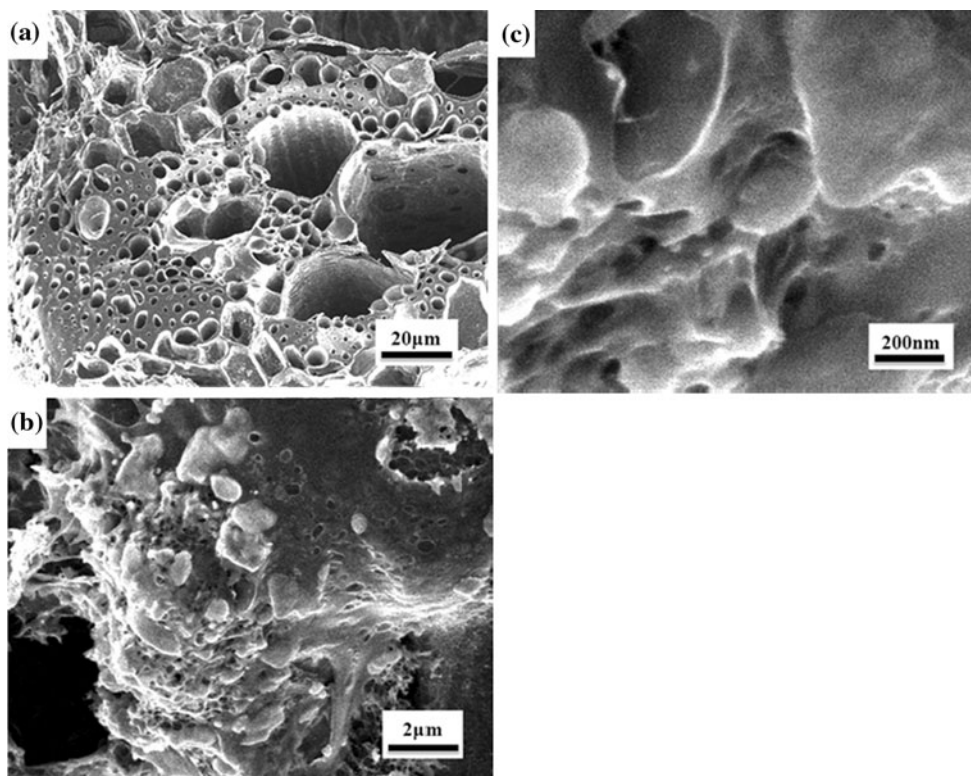

Fig. 6 X-ray diffraction pattern of PC-AC

Fig. 7 HRTEM image of the interior structure of the PC-AC

with optimum activation parameters attained a maximum S_{BET} value up to 2481 m^2/g with 1.21 cm^3/g pore volume. The disordered and isotropic structure of the AC consisted of curved and faceted graphitic layers with 1–2 nm in thickness and 5 nm in length. Typically, the crystallites contained 3–4 layers, enclosing randomly shaped pores with diameter less than 1 nm. Due to the tininess of the crystallite, there was interior strain in the lattice expanding the interlayer spacing of the AC to 0.370 nm. The A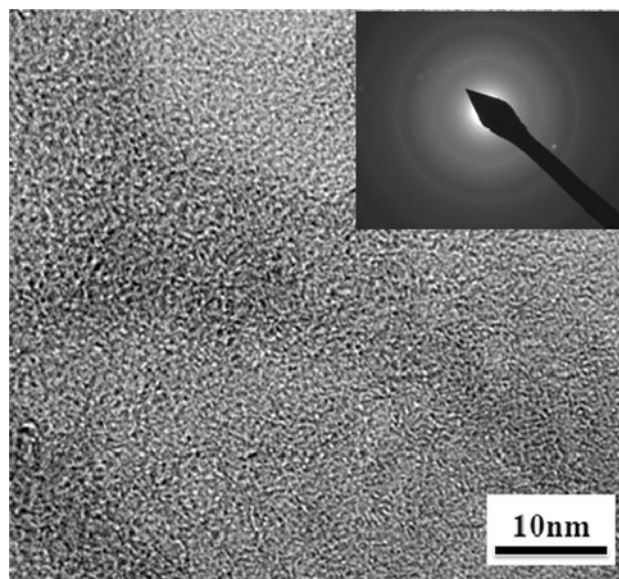C made from the *Zizania latifolia* leaves with one-step physical/chemical activation is expected to be economical, and used as a promising adsorbent for pollution control and other applications for its high surface area.

References

1. Azargohar R, Dalai AK (2008) Microporous Mesoporous Mater 110:413
2. Ismadji S, Bhatia SK (2001) Carbon 39:1237
3. Srinivasakannan C, Batar MZA (2004) Biomass Bioenergy 27:89
4. Wu FC, Tseng RL, Juang RS (2005) Sep Purif Technol 47:10
5. Wu FC, Tseng RL (2006) J Colloid Interface Sci 294:21
6. JY Gu, KX Li, Wang J, He HW (2010) Microporous Mesoporous Mater 131:393
7. Barrientos-Ramírez S, Oca-Ramírez GM, Sepúlveda-Escribano A, Pastor-Blas MM, González-Montiel A, Rodríguez-Reinoso F (2010) Catal Today 150:42
8. Bueres RF, Asedegbega-Nieto E, Díaz E, Ordóñez S, Díez FV (2010) Catal Today 150:16
9. Zhang T, Walter Walawender P, Fan LT, Fan M, Daugaard D, Brown RC (2004) Chem Eng J 105:53
10. Hayashi J, Horikawa T, Muroyama K, Gomes VG (2002) Microporous Mesoporous Mater 55:63
11. Guo Y, David A (2007) Microporous Mesoporous Mater 100:12
12. Adinata D, Ashri WM, Daud W, Aroua MK (2007) Bioresour Technol 98:145
13. Rajgopal S, Karthikeyan T, Prakashkumar BG, Miranda LS (2006) Chem Eng J 116:211
14. Sentorun-Shalaby Ç, Uçak-Astarlıoglu MG, Artok L, Sarıcı Ç (2006) Microporous Mesoporous Mater 88:126
15. Paraskeva P, Kalderis D, Diamadopoulos E (2008) J Chem Technol Biotechnol 83:581
16. Dias JM, Alvim-Ferraz MCM, Almeida MF, Rivera-Utrilla J, Sánchez-Polo M (2007) J Environ Manag 85:833
17. El-Hendawy AA, Samra SE, Girgis BS (2001) Colloids Surf A 180:209
18. Moreno-Castilla C, Carrosco-Marin F, Victoria-López-Ramon M, Alvarez-Merino MA (2001) Carbon 39:1415
19. Ichcho S, Khouya E, Fakhi S, Ezzine M, Hannache H, Pallier R, Naslain R (2005) J Hazard Mater 118:45
20. Okada K, Yamamoto N, Kameshima Y, Yasumori A (2003) J Colloid Interface Sci 262:179
21. Guo J, Lu AC (2003) Mater Chem Phys 80:114
22. Lu AC, Yang T (2004) J Colloid Interface Sci 274:594
23. Lillo-Rodenas MA, Juan-Juan J, Cazorla-Amoros D, Linares-Solano A (2004) Carbon 42:1371
24. Raymundo-Pinero E, Azais P, Cacciaguerra T, Cazorla-Amoros D, Linares-Solano A, Beguin F (2005) Carbon 43:786
25. Tsai WT, Chang CY, Lee SL (1998) Bioresour Technol 64:211
26. Karim MM, Das AK, Lee SH (2006) Anal Chim Acta 576:37
27. Gañan J, Gonza′lez-Garcı′a CM, Gonza′lez JF, Sabio E, Macı′as-Garcı′a A, Dı′az-Dı′ez MA (2004) Appl Surf Sci 238:347
28. Bansode RR, Losso JN, Marshall WE, Rao RM, Portier RJ (2003) Bioresour Technol 90:175
29. Walker PL Jr, Almagro A (1995) Carbon 33:239
30. Gergova K, Petrov N, Butuzova L, Minkova V, Isaeva L (1993) J Chem Technol Biotechnol 58:321
31. Yorgun S, Vurala N, Demirala H (2009) Microporous Mesoporous Mater 122:189
32. Olivares-Marín M, Fernández-González C, Macías-Garcia A, Gómez-Serrano V (2006) Appl Surf Sci 252:5980
33. Williams PT, Reed AR (2006) Biomass Bioenergy 30:144
34. Cuesta A, Mart′ınez-Alonso A, Tasco′n JMD, Bradley RH (1997) Carbon 35:967
35. Blanco Lo′pez MC, Mart′ınez-Alonso A, Tasco′n JMD (2000) Microporous Mesoporous Mater 34:171
36. Ishii C, Suzuki T, Shindo N, Kaneko K (1997) J Porous Mater 41:81
37. Kumar K, Saxena RK, Kothari R, Suri DK, Kaushik NK, Bohra JN (1997) Carbon 351:842
38. Carrott PJM, Nabais JMV, Ribeiro Carrott MML, Pajares JA (2001) Carbon 39:1543